


Longitudinal phase space dynamics of witness bunch during the Trojan Horse injection for plasma-based particle accelerators

Cite as: Phys. Plasmas **26**, 073103 (2019); <https://doi.org/10.1063/1.5108928>

Submitted: 04 May 2019 . Accepted: 11 June 2019 . Published Online: 15 July 2019

K. Moon , S. Kumar, M. Hur, and M. Chung



View Online



Export Citation



CrossMark



ULVAC

Leading the World with Vacuum Technology

- Vacuum Pumps
- Arc Plasma Deposition
- RGAs
- Leak Detectors
- Thermal Analysis
- Ellipsometers



Longitudinal phase space dynamics of witness bunch during the Trojan Horse injection for plasma-based particle accelerators

Cite as: Phys. Plasmas **26**, 073103 (2019); doi: 10.1063/1.5108928

Submitted: 4 May 2019 · Accepted: 11 June 2019 ·

Published Online: 15 July 2019



View Online



Export Citation



CrossMark

K. Moon,¹  S. Kumar,² M. Hur,¹ and M. Chung^{1,a)}

AFFILIATIONS

¹Department of Physics, Ulsan National Institute of Science and Technology, Ulsan 44919, South Korea

²Department of Physics, Manav Rachna University, Faridabad, Haryana 121004, India

^{a)}Electronic mail: mchung@unist.ac.kr

ABSTRACT

In the Trojan Horse injection process for plasma-based particle accelerators, we have investigated how the longitudinal phase space of the witness bunch would be governed by the parameters of the ionization laser and background plasma in the limit of quasistatic wakefield approximation. The tunneling ionization rate distribution by the laser pulse is introduced to describe the ionization time interval and initial distribution of the witness electrons. The quasilinear (or equivalently quasistatic) regime of the charged particle beam-driven wakefield is considered to make the phase of the wake potential constant in time in the driver beam frame. In the simulations, it is shown that the ionization laser phase on the quasistatic wake potential determines the longitudinal space-charge field of the witness bunch. We also find that the relative energy spread of the witness bunch can be estimated by the sum of three effects: The ionization time interval, wakefield slope, and space-charge fields of the witness bunch. Analytical expressions for the characteristic distance from the ionization to trapping positions, rms length, and relative energy spread of the witness bunch are obtained approximately and compared with the particle-in-cell simulations.

Published under license by AIP Publishing. <https://doi.org/10.1063/1.5108928>

I. INTRODUCTION

Since particle accelerators were first devised to discover new laws of physics, accelerator physicists have made continuous efforts to challenge the new energy frontiers. Indeed, in recent decades, there have been needs to construct even larger particle accelerators to reach beam energies higher than ever achieved, particularly for the lepton collider experiments. Conventional accelerators based on radio frequency (RF) cavities have limitations in accelerating gradients (~ 100 MV/m), and thus, the new accelerators would be very expensive and have large footprints. On the other hand, advanced accelerators based on novel acceleration mechanisms, such as the plasma wakefield accelerators, are expected to have much higher accelerating gradients and could save the cost and footprints of the collider experiments considerably. Plasma wakefields can be generated by injecting a high intensity laser pulse or charged particle beam into a plasma.^{1,2} Strong electric fields of the plasma wakefields guarantee the accelerating and focusing forces orders of magnitudes larger than the conventional accelerators. However, there remain several issues for the practical use of the plasma wakefield accelerators, such as difficulties of staging,³

unstable propagation of drivers,⁴ substantial energy spread,⁵ and emittance growth of witness bunch,⁶ to mention a few of them. For the successful injection of the witness bunch into the accelerating wakefield region of an ion cavity, its normalized transverse and longitudinal sizes are required to be much smaller than unity, $k_p \sigma \ll 1$, where $k_p = \sqrt{n_0 e^2 / \epsilon_0 m_e c^2}$ is the plasma wave number. Because of the complicated physics of transverse phase space matching between the witness beam and plasma, even the plasma density profile at the beam entrance is of a serious concern.⁵ In this regard, novel injection techniques for controllable witness bunch parameters have been actively proposed recently.^{7–11}

The Trojan Horse (TH) injection method uses a laser pulse with a small normalized vector potential ($a_i \ll 1$) to ionize the residual gas inside the accelerating region of the plasma wakefield induced by a dense ($n_0 \ll n_{b0}$) driver beam.^{8,12,13} Here, n_0 is the plasma density and n_{b0} is the peak driver beam density. This TH injection method makes it possible to separate the physics of the driver and witness beams. We note, in contrast, that the ionization injection process by a driver beam only is closely coupled to the driver beam parameters. For the parameters of interest, the TH injection could deliver the accelerating fields

around the wave-breaking limit E_0 (V/cm) $\propto \sqrt{n_0}$ (cm⁻³) and the witness beams with tens of nm transverse emittances and a few kA of peak currents.

Nevertheless, the needs of state-of-the-art technologies such as the spatiotemporal alignment on micrometer and femtosecond scales, ultrahigh driver beam current capability, tunable multicomponent gas mixtures, selective optical ionization, wide enough plasma channels without any harmful boundary effects, and others have delayed the successful realization of the TH injection.¹⁴ As an example of the extreme synchronism requirement between the driver beam and ionization laser pulse in the TH injection method, we note that the timing jitter should be less than ~ 20 fs for the beam and laser parameters considered in this study. By carefully designing a laser beam splitter and the use of a high-precision delay line, one might achieve such a level of timing jitter requirement in the actual experimental setup. In addition to these challenges in experimental setups, the significant energy spread of the witness bunch inherent in the ultrahigh accelerating field gradient still matters. A novel approach for orders of magnitude smaller witness bunch energy spread has been reported,¹³ and in this work, we investigate further on this inherent energy spread issue. Since the phase of the plasma response from the driver beam oscillates with a high frequency $\omega \gg 2\pi c/Z_R$, where Z_R is the Rayleigh length of the ionization laser, the energy spread of the witness bunch is affected by the phase oscillation amplitude of the plasma response, which can be much larger than the rms length of the tunneling ionization rate distribution of the laser pulse. In this paper, we call this phenomenon the wakefield jitter effect. In order to relax these limitations, we consider the possibility of using parameters with enlarged system scales¹⁴ and also investigate the strict condition for the quasistatic approximation to be valid, which would minimize the rms length increase in the witness bunch.

In Sec. II, the overall strategy of the TH injection is explained. The mixture of hydrogen and helium gases is used for the media of the plasma wakefield and the source of the witness electrons. The ionization rate distribution by the laser pulse is introduced, and the initial intrinsic energy spread during the ionization process is obtained. In Sec. III, the plasma wakefield and its potential in the ultrarelativistic blowout regime are briefly explained. It is reminded that the wake potential for trapping of the witness electron is indeed scale-free for given normalized beam sizes (by k_p^{-1}) and current in the ultrarelativistic blowout regime.¹⁵ Also, the selection criteria of the driver beam and plasma parameters are investigated to avoid the wakefield jitter effects. In Sec. IV, based on the concepts developed in Secs. II and III, the analytical expressions for the trapping condition and rms length are introduced to estimate the relative energy spread of the witness bunch. It is demonstrated that these analytical expressions for the witness bunch properties⁹ are in reasonable agreement with the simulation results from the FBPIC (Fourier–Bessel particle-in-cell) code.¹⁶

For the simulations of the TH injection, the parameters for the ultrarelativistic regime are set as follows: The plasma density $n_0 = 9.0 \times 10^{16}$ cm⁻³, driver beam density $n_{b0} = 4.0 \times 10^{17}$ cm⁻³, average driver beam particle energy $\langle E_d \rangle = 10$ GeV, normalized driver beam sizes $k_p \sigma_{b,z} = 1.3$ and $k_p \sigma_{b,r} = 0.5$, and driver beam normalized transverse emittance $\epsilon_r = 15$ μ m. The dimensions of the ionization laser pulse are set to the focal waist $w_i = 8$ μ m and rms length $L_i = 12$ μ m. In order to save the computing resources, the simulations were performed based on the boosted-frame technique with the relativistic

gamma of the boosted-frame $\gamma_{boost} = 2$. The resolution of the simulation is set to $\Delta z = \lambda_i/20$, $\Delta r = \lambda_i/5$, and $\Delta t = \Delta z/c$ in the laboratory frame with the ionization laser wavelength of $\lambda_i = 0.8$ μ m. Due to the spectral solver used in the FBPIC code, our simulation has no Courant limit and guarantees the intrinsic mitigation of Numerical Cherenkov Radiation (NCR) from relativistic bunches.¹⁶

II. TROJAN HORSE INJECTION SCENARIO

In the original proposal for the TH injection, the lithium (Li) and helium (He) gas mixture was used,⁸ where lithium is the lower-ionization-threshold (LIT) component and helium is the higher-ionization-threshold (HIT) component. Since helium is not supposed to be ionized at the ionization threshold of lithium, helium can exist in the accelerating wakefield region of the lithium plasma. In this paper, the mixture of hydrogen (H) and helium gases was considered. It is assumed that the neutral hydrogen gas is preionized by a laser pulse which has a waist and a duration much larger than λ_p and normalized vector potential $0.027 < a_{pre} \ll 0.067$ which is just high enough to ionize only the hydrogen and helium gases (but not the helium ions). The number density of the plasma electrons is set to $n_0 = 9.0 \times 10^{16}$ cm⁻³, and the number density of He gas is set to $n_{He} = 0.02n_0$ [Fig. 1(b)]. In this case, the mismatching of the focal strength at the boundary of the HIT gas region is negligible.

The He⁺ ions are ionized by another laser pulse which follows the driver beam. The ionization laser pulse is focused at the focal point z_f , which is inside the first bucket of the accelerating region of the plasma wakefield and has a waist and a duration much smaller than λ_p [Fig. 1(b)]. To ionize He⁺ to He²⁺, the ionization laser pulse should have the normalized vector potential $a_i (=0.067)$ larger than that of the preionizing laser. The tunneling ionization rates of hydrogen and helium atoms are given by the ADK theory¹⁷ as shown in Fig. 1(a).

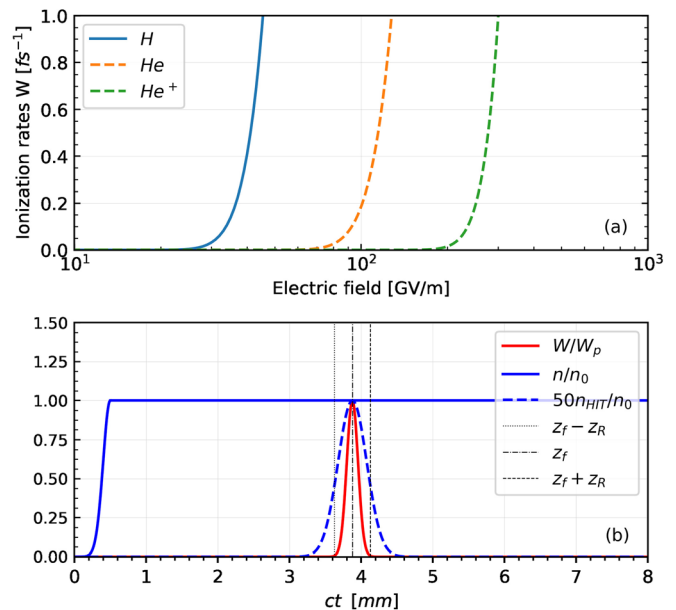


FIG. 1. (a) The tunneling ionization rates (W) of hydrogen and helium atoms and (b) the gas density profiles (n and n_{HIT}) with the ionization rate distribution of the Gaussian laser pulse. The ionization laser pulse is focused at $z_f \approx 3878$ μ m.

Around the centroid and focal point of the ionization laser pulse, the distribution of the tunneling ionization rate is given by the Keldysh theory, which is written in the form^{9,18}

$$W \approx W_p \exp \left[-\frac{(z - z_f)^2}{2\sigma_\psi^2 Z_R^2} \right] \times \exp \left[-\frac{r^2}{\sigma_\psi^2 w_i^2} \right] \exp \left[-\frac{(\xi - \langle \xi_i \rangle)^2}{2\sigma_\psi^2 L_i^2} \right], \quad (1)$$

with

$$\sigma_\psi \approx \left(\frac{3\pi r_e a_i}{\alpha^4 \lambda_i} \right)^{1/2} \left(\frac{U_H}{U_I} \right)^{3/4}, \quad (2)$$

where W_p is the tunneling ionization rate at the peak of the laser field, σ_ψ is the rms spread in the injection laser phase, $\xi = z - ct$ is the comoving variable in the beam frame, $\langle \xi_i \rangle$ is the centroid of the laser pulse, r_e is the classical electron radius, α is the fine structure constant, U_H is the ionization potential of hydrogen, and U_I is the ionization potential of the HIT particle. To ensure that Eq. (2) is valid, it is assumed that the laser field amplitude is set to the ionization threshold $(\lambda_i/c)W_p \lesssim 1$ and $\sigma_\psi^2 \ll 1$. The intrinsic energy spread which is generated during the trapping process is determined by $\sigma_{E_i} = eE_{z,t} \sigma_\psi Z_R$, with $Z_R \approx 251 \mu\text{m}$ and $\sigma_\psi \approx 0.31$, where $E_{z,t}$ is the accelerating wakefield at the phase of the trapping. A similar term was also derived in Ref. 13, but the estimation we suggest here contains additional dependencies on the laser-plasma parameters based on Keldysh theory.

III. QUASILINEAR REGIME OF BEAM-DRIVEN PLASMA WAKEFIELDS

When a relativistic charged particle beam propagates through the plasma, the static field of the beam space-charge displaces the plasma electrons. The displaced electrons are then pulled back by the restoring force of the stationary ions. Therefore, the plasma electrons oscillate around the initial equilibrium positions after the driving charged particle beam passes through. In the limit $n_{b0} \ll n_0$, the amplitudes of the displaced plasma electrons are usually very small ($k_p |r_1| \ll 1$). Hence, in this case, the fluid model can be reduced to the linear theory, and the mathematical dependencies of the perturbed parameters are given in terms of the sinusoidal functions.² On the other hand, in the regime $n_{b0} \gg n_0$, the magnitudes of the perturbed quantities become very large and the fluid model breaks down.^{19–21} The maximum blowout radius r_m is determined by the normalized charge per unit length of the driver beam $\Lambda \equiv (n_{b0}/n_0)k_p^2 \sigma_{b,r}^2$.^{20,21} Particularly, for the case $k_p r_m \gg 1$, which corresponds to a pure ion channel around the center of the wake potential, the plasma wakefields and their static potential in the laboratory frame are given as^{20–22}

$$(E_r - cB_\theta)/E_0 \approx k_p r/2, \quad (3)$$

$$E_z/E_0 \approx k_p (\xi - \xi_0)/2, \quad (4)$$

and

$$e\Delta\Phi/m_e c^2 \approx k_p^2 [\Delta\xi^2 + 2\Delta\xi(\xi_i - \xi_0)]/4, \quad (5)$$

where $E_0 = k_p m_e c^2/e$ is the wave-breaking limit in cold plasma,¹⁹ $\Delta\xi = \xi_t - \xi_i$ is the characteristic distance from the ionization to trapping positions of the witness electrons, and the relative beam

coordinates ξ with subscripts 0, t , and i indicate the peak of the wake potential, trapping, and ionization positions of the witness electrons, respectively. For the wakefield region of interest, we have $\xi < \xi_0$.

The electromagnetic potential is defined by $\Psi \equiv \Phi - v_\phi A_z$, where $v_\phi (\approx c)$ is the phase velocity of the wake. Ψ is related to the electromagnetic fields by $E_z = -\partial_\xi \Psi$ and $E_r - v_\phi B_\theta = -\partial_r \Psi$. The transverse wakefield $E_r - cB_\theta$ near the axis ($k_p r \ll 1$ or $k_p x \ll 1$) has the linearity and dependence only on r , not z [see Figs. 2(a) and 2(d)]. Similarly, the longitudinal wakefield E_z nearby the peak of wake potential (Ψ) has the linearity and dependence only on z , not r . In Fig. 2(f), two vertical lines are drawn to indicate the centroid positions of the ionization laser pulse ($\langle \xi_i \rangle$) and witness bunch ($\langle \xi_t \rangle$). When $k_p r_m \sim 2$, we note $\partial_r(E_r - cB_\theta) \neq \partial_\xi E_z$ and $\partial_\xi E_z < k_p E_0/2$, which is the case for our simulation (Fig. 2). Since the effectiveness of inducing plasma waves is determined by Λ and $\sigma_{b,z}$,²⁰ the curves of wakefields as a function of the beam coordinate ξ normalized by the plasma skin depth k_p^{-1} are identical for fixed Λ and $\sigma_{b,z}$ even with varying ambient plasma densities n_0 ¹⁵ (see Fig. 3). This means that the trapping condition of the witness electrons for the TH injection remains the same for the given normalized beam sizes and current. Hence, we may consider the use of enlarged system scales to relax extremely tight experimental conditions for the TH injection scenario.

It is worthwhile to mention the condition in which the quasistatic approximation is valid for the electromagnetic potential. The high-current driver beam makes the peak position of the wake potential ξ_0 oscillate in time.^{21,23} Even though the plasma electrons displaced by the driver beam predominantly oscillate in the transverse directions, still there are some residual longitudinal oscillations. When the self-injected plasma current becomes large enough to generate a strong azimuthal magnetic field which can distort the plasma sheath at the rear part of the ion cavity, the phase of the wake potential oscillates in time (see Fig. 4). If the phase of the plasma response oscillates as $\xi_0 = \xi_{00} + \xi_{01} \exp(i\omega t)$ with the amplitude $\sigma_\psi L_i/2 \ll \xi_{01} \ll \xi_{00}$ and frequency $\omega \gg 2\pi c/Z_R$, then the multiple peaks of the witness beam current will be generated. In this case, we have $\sigma_z \sim \xi_{01}$, causing large energy spread of the witness beam. The details of the energy spread issues for large Λ values will be investigated in the future work. For the present simulation study, we have $\lambda_p \approx 111 \mu\text{m}$ and $k_p r_m \approx 2.4$ ($\Lambda = 1.1$), which makes Eqs. (3) and (4) satisfied approximately with negligible self-injected plasma current effects.

IV. MANIPULATION OF THE WITNESS BUNCH LONGITUDINAL PHASE SPACE

Assuming a quasistatic electromagnetic potential, the ionized witness electrons can be trapped into the accelerating wakefield region at the expense of electromagnetic wake potential $e\Delta\Psi/m_e c^2 \approx 1$. Using Eq. (5) and setting the ionization laser pulse near the maximum position of wake potential ($\xi_i \sim \xi_0$), $\Delta\xi$ can be written in the form

$$k_p \Delta\xi \approx -k_p (\xi_i - \xi_0) - \sqrt{k_p^2 (\xi_i - \xi_0)^2 + 2E_0/\partial_{k_p \xi} E_{z,i}}, \quad (6)$$

where it is assumed that the ionization laser pulse has no transverse offset with respect to the propagation axis of the driver electron beam and $\partial_{k_p \xi} E_z$ is constant within $\xi_t < \xi < \xi_i$. A formula similar to Eq. (6) has been reported in Ref. 24, but in Eq. (6), the first term is additionally corrected and the second term in the square root has been modified for the quasilinear wakefield regime.

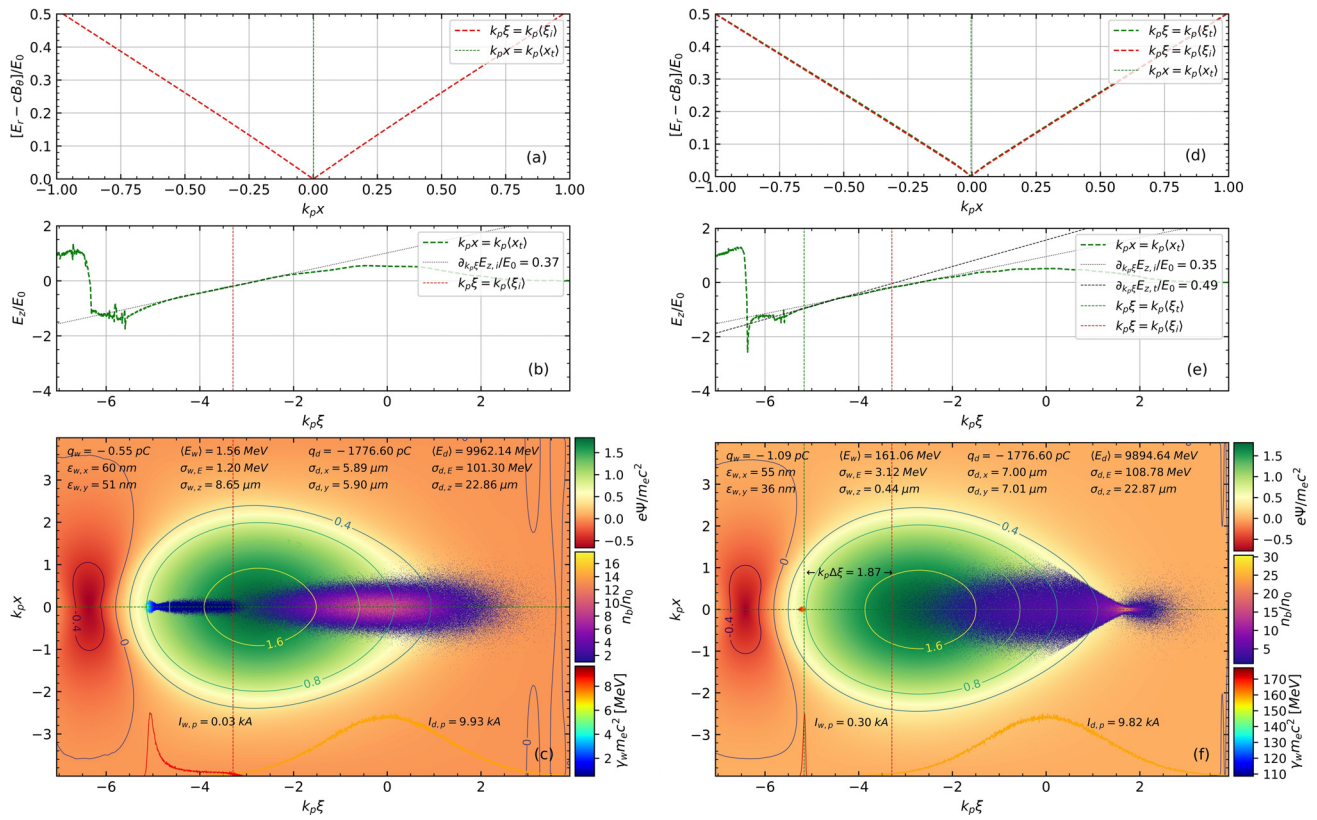


FIG. 2. The plasma wakefields acting on the beams at (left) $ct = 4$ mm and (right) $ct = 10$ mm for $k_p \langle \xi_i \rangle = -3.3$. [(a) and (d)] $(E_r - cB_\theta)/E_0$ along the vertical lines at $\langle \xi_i \rangle$ (green dotted) and $\langle \xi_i \rangle$ (red dotted). [(b) and (e)] E_z/E_0 along the horizontal line at $x = \langle x_i \rangle = 0$. [(c) and (f)] The two-dimensional plots of the wake potential distribution, $e\psi/m_e c^2$. The vertical lines are set to the longitudinal positions of the witness bunch centroids and ionization laser pulses. The horizontal lines are set to the transverse positions of the witness bunch centroids. All the coordinate axes are normalized by the plasma skin depth k_p^{-1} . The energy of the witness bunch is given by $\gamma_w m_e c^2$ (mega-electron-volt). The driver beam is moving to the right.

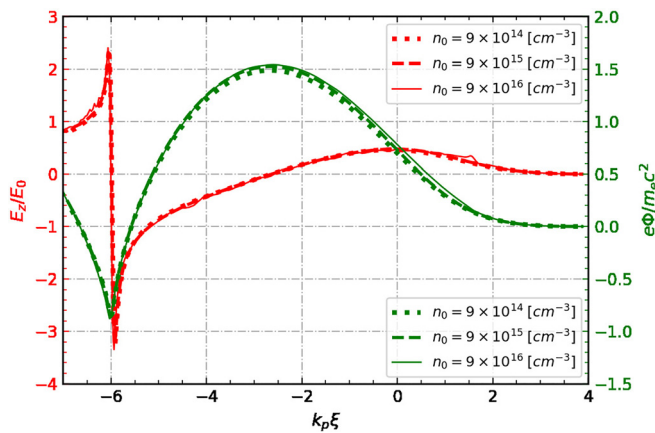


FIG. 3. (red curves) The longitudinal components of plasma wakefields and (green curves) their potentials for $k_p \sigma_{b,r} = 0.5$, $k_p \sigma_{b,z} = 1.3$, and $\Lambda = 1$. The driver beam is moving to the right.

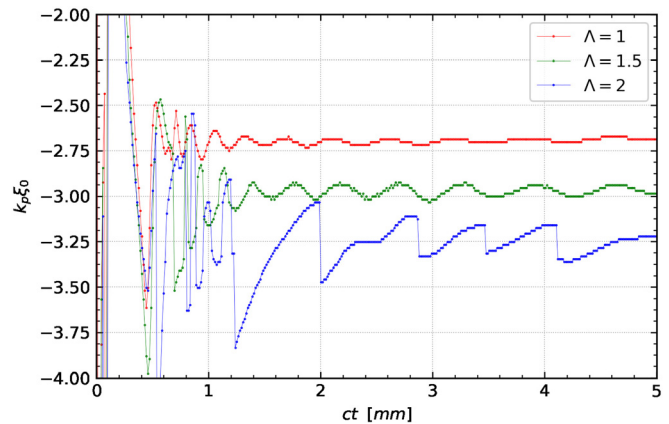


FIG. 4. The peak positions (ξ_0) of wake potentials in the comoving coordinate, which are defined as the relative distances from the driver beam centroids ($\xi = 0$) to the peaks of wake potentials, oscillate along the propagation distance $z = ct$ for $k_p \sigma_{b,z} = 1.3$ and $n_0 = 9 \times 10^{16} \text{ cm}^{-3}$.

When the quasistatic approximation is valid, the rms length of the witness bunch is estimated by Eqs. (1), (5), and (6), namely,

$$\sigma_z \approx \left(|\langle \xi_i \rangle - \xi_0| + \frac{\sigma_{\psi} L_i}{2} \right) \left(1 + \frac{\langle \xi_i \rangle - \xi_0}{|\Delta \xi|} \right) \frac{\sigma_{\psi} L_i}{|\Delta \xi|}, \quad (7)$$

where L_i is the rms length of the ionization laser pulse. It is assumed that the intrinsic transverse momentum induced in the laser polarization direction is negligible in Eq. (7) because its effect in the trapping process is inversely proportional to the wake phase velocity gamma γ_p which is close to the driver beam gamma γ_d .²⁵ Equation (7) confirms that the rms length of the witness bunch is minimized when the ionization laser pulse is set to the peak of the wake potential (see Fig. 5). We note, however, that Eq. (7) is not perfectly matched to the simulation results quantitatively. It is because for the majority of cases in the quasistatic approximation, the witness electrons reach the nonlinear curve of E_z at the rear part of the ion cavity, particularly when the ionization laser is set far from $k_p \xi_0$. This shortens the rms length of the witness bunch from the analytical expectation of Eq. (7).

Assuming that the phase slippage of the witness bunch on the wake potential is negligible after the trapping process is performed, the energy spread of the witness bunch can be estimated by the combination of three effects: The intrinsic energy spread from the ionization time interval, work done by the wakefield slope, and longitudinal space-charge field of the witness bunch. The energy spread from the wakefield slope during the acceleration process is given by $\sigma_{E,a} \approx e \sigma_z (z - z_0) \partial_{\xi} E_{z,t}$ where $z_0 = z_f + \sqrt{\pi/2} \sigma_{\psi} Z_R$ is the virtual point in which the witness bunch charge is accumulated up to almost N . Here, $N \approx \pi (\sigma_{\psi} w_i)^2 (\sqrt{2\pi} \sigma_{\psi} Z_R) n_{\text{HTT}}$ is the maximum number of ionized witness electrons.⁹ The energy spread $\sigma_{E,s}$ from the longitudinal space charge field is approximately given by²⁶

$$\sigma_{E,s} \approx e \int_{z_0}^z E_{z,s} dz', \quad (8)$$

with

$$E_{z,s} \approx \frac{N}{4\pi\epsilon_0} \frac{e}{\gamma^2 \sigma_z^2} \log \frac{\gamma \sigma_z}{\sigma_r}, \quad (9)$$

where $\gamma = \gamma_i + eE_{z,t}(z - z_0)/m_e c^2$ is the relativistic gamma of the accelerating witness bunch, γ_i is the initial gamma of the witness bunch at $z = z_0$, and σ_r is the witness bunch radius. By the initial matching condition $k_p w_i \sim 2a_p$,⁹ the witness bunch radius in the laser polarization direction is approximately matched to $\sigma_r = \sqrt{\epsilon_r/\gamma} k_{\beta}$ with the betatron wave number $k_{\beta} = k_p/\sqrt{2\gamma}$.²⁷ Since the contribution of the $\sigma_z \sigma_r^{-1}$ term becomes quickly small compared to γ , it can be assumed that the possible mismatching effect of the witness bunch radius is not significant for the relative energy spread [see Eq. (10)]. The average energy of the witness bunch is $\langle E \rangle = \gamma_i m_e c^2 + eE_{z,t}(z - z_0) \approx eE_{z,t}(z - z_0)$, where it was assumed that the initial witness bunch energy is negligible.

Reminding that the intrinsic energy spread $\sigma_{E,i}$ determines the size of the semiminor axis of the longitudinal phase space ellipse and the forces acting on the witness bunch in the opposite directions affect the tilt angle of the semi-major axis, we suggest the following expression for the relative energy spread of the witness bunch:

$$\begin{aligned} \frac{\sigma_E}{\langle E \rangle} &\approx \frac{\sigma_{E,i} + |\sigma_{E,a} + \sigma_{E,s}|}{\langle E \rangle}, \\ &\approx \frac{\sigma_{\psi} Z_R}{z - z_0} + \left| \frac{1}{E_{z,t}} \frac{\partial E_{z,t}}{\partial \xi} \sigma_z - \frac{N}{4\pi\epsilon_0} \frac{e^2}{\sigma_z} (eE_{z,t} \sigma_z)^{-1} \right. \\ &\quad \left. \times \left\{ \frac{\log(\gamma \sigma_z \sigma_r^{-1}) + 1.25}{\gamma^2} - \frac{\log(\gamma_i \sigma_z \sigma_{r,i}^{-1}) + 1.25}{\gamma \gamma_i} \right\} \right|, \quad (10) \end{aligned}$$

where σ_E is the total rms energy spread of the witness bunch and $\sigma_{r,i}$ is the initial witness bunch radius. It is assumed that any wakefield effect driven by the witness bunch itself is negligible in the present TH

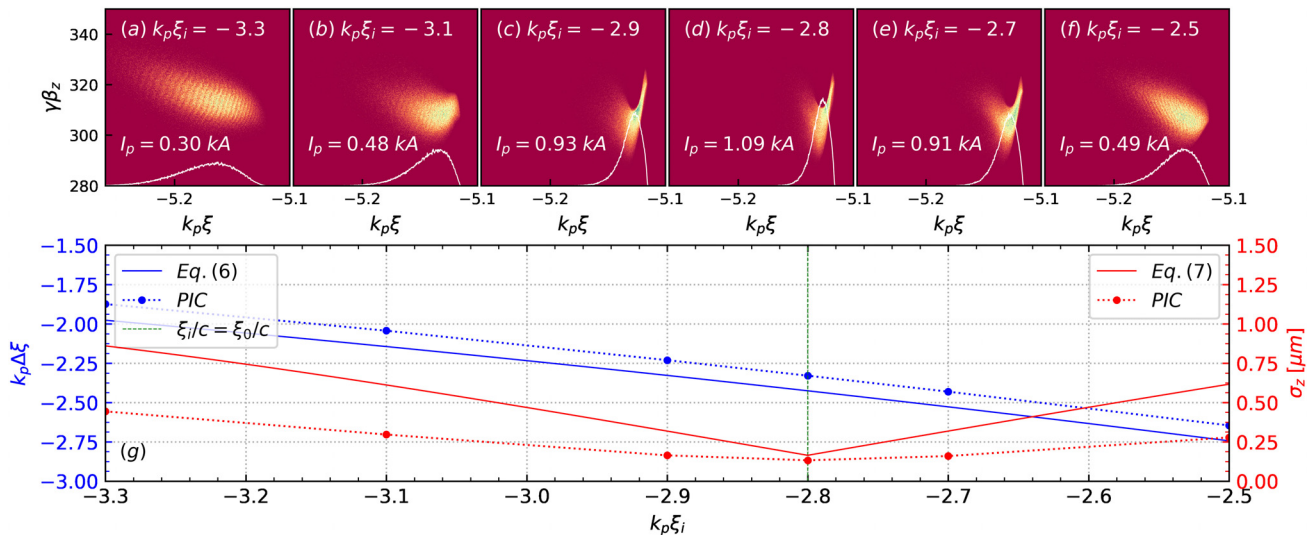


FIG. 5. [(a)–(f)] The longitudinal phase spaces of the witness bunch with different ionization phases for $\partial_{k_p \xi} E_{z,t}/E_0 \sim 0.34$ and $ct = 10$ mm. (g: Blue) The characteristic distance from the ionization to trapping positions and (g: Red) the rms length of the witness bunch, according to the different phases of the ionization laser pulse $k_p \xi_i$ on the quasistatic wake potential. Here, the peak position of the wake potential is $k_p \xi_0 = -2.8$, which corresponds to ~ 160 fs behind the driver beam centroid ($\xi = 0$).

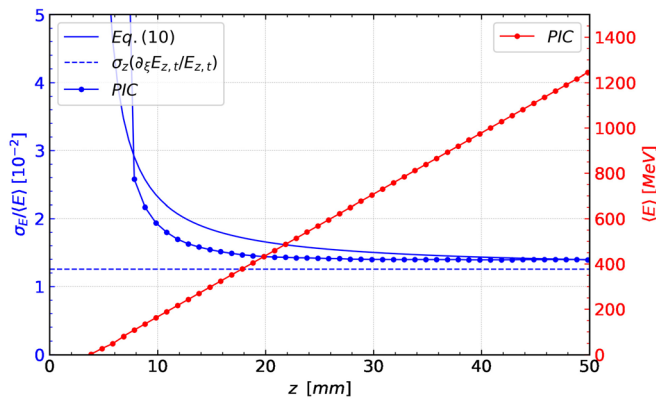


FIG. 6. The average energy and energy spread of the witness bunch for $k_p \xi_i = -3.3$ (blue dashed line) The asymptotic behavior of the relative energy spread. (blue solid curve) The analytical expression (10) for the relative energy spread. (blue circles) The PIC simulation result of the relative energy spread. (red circles) The PIC simulation result of the average energy.

injection regime. For the case in which the ionization laser pulse is synchronized near the peak position of the wake potential, $E_{z,t}$ and $\partial_z E_{z,t}$ are specified by E_0 and $k_p E_0/2$, respectively. We note that $\sigma_{E,i}$ and $\sigma_{E,s}$ of Eq. (10) are comparable to $\sigma_{E,a}$ at $ct = 10$ mm in Fig. 5. Due to the high bunch density, Figs. 5(a)–5(f) illustrate that the energy chirp of the witness bunch is space-charge field dominated when the ionization laser is synchronized near the peak position of the wake potential at $k_p \xi_0 = -2.8$, whereas it is plasma-wakefield dominated when the ionization laser is synchronized far from $k_p \xi_0$. Equation (10) implies $\sigma_E / \langle E \rangle \propto n_0$ at $z \rightarrow \infty$, where the effects of $\sigma_{E,i}$ and $\sigma_{E,s}$ vanish. A partly similar simulation result as in Fig. 6 has been reported in Ref. 13. In Ref. 13, a high-charge escort bunch was additionally injected to distort the wakefield gradient. In this work, instead, we tried to figure out the minimization condition of the rms length and considered the self-field effect⁵ of the witness bunch. The simulation result of the relative energy spread in Fig. 6 shows a reasonable agreement with Eq. (10) (compare blue circles and the blue dashed line in Fig. 6).

V. SUMMARY

In this work, the Trojan Horse injection scheme has been revisited in the limit where the plasma wave jitter effect is negligible. For the ultrarelativistic blowout regime, it was found that the trapping condition of the witness electrons has no absolute dependence on the plasma density. Therefore, it could be possible to reproduce the TH injection systems of similar characteristics with drastically different plasma densities and length scales. The rms length of the witness bunch is minimized when the laser pulse is set near the peak position of the wake potential distribution. The shorter rms length of the witness beam leads to the smaller asymptote of the relative energy spread, unless the space-charge field of the witness bunch is significant. The smaller ambient plasma density (n_0) guarantees not only the relaxed requirement of the synchronism ($k_p |\xi_i - \xi_0| \leq 0.5$) but also the improved relative energy spread of the witness bunch ($\sigma_E / \langle E \rangle \propto n_0$). The analytical expressions introduced in this work

show reasonably similar trends to the PIC simulation results and should be useful for quick assessment of the TH injection systems.

ACKNOWLEDGMENTS

We thank people of the BLAST program at LBNL for their help in the FBPIC code. This work was supported by the National Research Foundation of Korea (Grant Nos. NRF-2016R1A5A1013277 and NRF-2017M1A7A1A02016413).

REFERENCES

- ¹T. Tajima and J. M. Dawson, *Phys. Rev. Lett.* **43**, 267 (1979).
- ²P. Chen, J. M. Dawson, R. W. Huff, and T. Katsouleas, *Phys. Rev. Lett.* **54**, 693 (1985).
- ³X. L. Xu, J. F. Hua, Y. P. Wu, C. J. Zhang, F. Li, Y. Wan, C. H. Pai, W. Lu, W. An, P. Yu, M. J. Hogan, C. Joshi, and W. B. Mori, *Phys. Rev. Lett.* **116**, 124801 (2016).
- ⁴W. An, M. Zhou, N. Vafaei-Najafabadi, K. A. Marsh, C. E. Clayton, C. Joshi, W. B. Mori, W. Lu, E. Adli, S. Corde, M. Litos, S. Li, S. Gessner, J. Frederico, M. J. Hogan, D. Walz, J. England, J. P. Delahaye, and P. Muggli, *Phys. Rev. Spec. Top. Accel. Beams* **16**, 101301 (2013).
- ⁵M. Tzoufras, W. Lu, F. S. Tsung, C. Huang, W. B. Mori, T. Katsouleas, J. Vieira, R. A. Fonseca, and L. O. Silva, *Phys. Rev. Lett.* **101**, 145002 (2008).
- ⁶R. Gholizadeh, T. Katsouleas, P. Muggli, C. Huang, and W. Mori, *Phys. Rev. Lett.* **104**, 155001 (2010).
- ⁷E. Oz, S. Deng, T. Katsouleas, P. Muggli, C. D. Barnes, I. Blumenfeld, F. J. Decker, P. Emma, M. J. Hogan, R. Ischebeck, R. H. Iverson, N. Kirby, P. Krejcik, C. O'Connell, R. H. Siemann, D. Walz, D. Auerbach, C. E. Clayton, C. Huang, D. K. Johnson, C. Joshi, W. Lu, K. A. Marsh, W. B. Mori, and M. Zhou, *Phys. Rev. Lett.* **98**, 084801 (2007).
- ⁸B. Hidding, G. Pretzler, J. B. Rosenzweig, T. Konigstein, D. Schiller, and D. L. Bruhwiler, *Phys. Rev. Lett.* **108**, 035001 (2012).
- ⁹C. B. Schroeder, J.-L. Vay, E. Esarey, S. S. Bulanov, C. Benedetti, L. L. Yu, M. Chen, C. G. R. Geddes, and W. P. Leemans, *Phys. Rev. Spec. Top. Accel. Beams* **17**, 101301 (2014).
- ¹⁰A. Martinez de la Ossa, J. Grebenyuk, T. Mehrling, L. Schaper, and J. Osterhoff, *Phys. Rev. Lett.* **111**, 245003 (2013).
- ¹¹A. Martinez de la Ossa, Z. Hu, M. J. V. Streeter, T. J. Mehrling, O. Kononenko, B. Sheeran, and J. Osterhoff, *Phys. Rev. Accel. Beams* **20**, 091301 (2017).
- ¹²Y. Xi, B. Hidding, D. L. Bruhwiler, G. Pretzler, and J. B. Rosenzweig, *Phys. Rev. Spec. Top. Accel. Beams* **16**, 031303 (2013).
- ¹³G. G. Manahan, A. F. Habib, P. Scherkl, P. Delinikolas, A. Beaton, A. Knetsch, O. Karger, G. Wittig, T. Heinemann, Z. M. Sheng, J. R. Cary, D. L. Bruhwiler, J. B. Rosenzweig, and B. Hidding, *Nat. Commun.* **8**, 15705 (2017).
- ¹⁴B. Hidding, G. G. Manahan, T. Heinemann, P. Scherkl, F. Habib, D. Ullmann, A. Beaton, A. Sutherland, A. Knetsch, O. Karger, G. Wittig, B. O'Shea, V. Yakimenko, M. Hogan, S. Green, C. Clarke, S. Gessner, J. B. Rosenzweig, A. Deng, M. Litos, D. L. Bruhwiler, J. Smith, J. R. Cary, R. Zgadzaj, M. C. Downer, C. Lindstrom, E. Adli, and G. Andonian, "First measurements of Trojan horse injection in a plasma wakefield accelerator," in Proceedings of the IPAC (2017), p. TUYB1.
- ¹⁵W. Lu, C. Huang, M. Zhou, W. B. Mori, and T. Katsouleas, *Phys. Plasmas* **12**, 063101 (2005).
- ¹⁶R. Lehe, M. Kirchen, I. A. Andriyash, B. B. Godfrey, and J.-L. Vay, *Comput. Phys. Commun.* **203**, 66–82 (2016).
- ¹⁷D. L. Bruhwiler, D. A. Dimitrov, J. R. Cary, E. Esarey, W. Leemans, and R. E. Giacone, *Phys. Plasmas* **10**, 2022 (2003).
- ¹⁸V. S. Popov, *Phys. Usp.* **47**, 855 (2004).
- ¹⁹J. B. Rosenzweig, *Phys. Rev. Lett.* **58**, 555 (1987).
- ²⁰W. Lu, C. Huang, M. Zhou, W. B. Mori, and T. Katsouleas, *Phys. Rev. Lett.* **96**, 165002 (2006).
- ²¹W. Lu, C. Huang, M. Zhou, M. Tzoufras, F. S. Tsung, W. B. Mori, and T. Katsouleas, *Phys. Plasmas* **13**, 056709 (2006).

- ²²E. Esarey, C. B. Schroeder, and W. P. Leemans, *Rev. Mod. Phys.* **81**, 1229 (2009).
- ²³K. V. Lotov, *Phys. Rev. E* **69**, 046405 (2004).
- ²⁴X. L. Xu, J. F. Hua, F. Li, C. J. Zhang, L. X. Yan, Y. C. Du, W. H. Huang, H. B. Chen, C. X. Tang, W. Lu, P. Yu, W. An, C. Joshi, and W. B. Mori, *Phys. Rev. Lett.* **112**, 035003 (2014).
- ²⁵M. Chen, E. Esarey, C. B. Schroeder, C. G. R. Geddes, and W. P. Leemans, *Phys. Plasmas* **19**, 033101 (2012).
- ²⁶G. Stupakov and P. Gregory, *Classical Mechanics and Electromagnetism in Accelerator Physics* (Springer, 2018), pp. 141–144.
- ²⁷E. Esarey, B. A. Shadwick, P. Catravas, and W. P. Leemans, *Phys. Rev. E* **65**, 056505 (2002).